

## Supporting Information

### Tetrazine- and *trans*-Cyclooctene-functionalised Polypept(o)ides for Fast Bioorthogonal Tetrazine Ligation

Kerstin Johann,<sup>a</sup> Dennis Svatunek,<sup>b</sup> Christine Seidl,<sup>a</sup> Silvia Rizzelli,<sup>a</sup> Tobias Bauer,<sup>a</sup> Lydia Braun,<sup>a</sup> Kaloian Koynov,<sup>c</sup> Hannes Mikula<sup>b</sup> and Matthias Barz<sup>\*a</sup>

<sup>a</sup> Department of Chemistry, Johannes Gutenberg University Mainz, Duesbergweg 10-14, 55128 Mainz, Germany.

<sup>b</sup> Institute of Applied Synthetic Chemistry, Technische Universität Wien, Getreidemarkt 9, 1060 Vienna, Austria.

<sup>c</sup> Max Planck Institute for Polymer Research, Ackermannweg 10, 55128 Mainz, Germany.

## 1. Experimentals

### 1.1. Monomer syntheses

**Sarcosine *N*-carboxyanhydride.** Sarcosine *N*-carboxyanhydride (Sar NCA) was synthesised as previously reported.<sup>1</sup> Sarcosine (14.6 g, 0.16 mol) was dried *in vacuo* in a flame-dried, 500 mL three-necked round bottom flask overnight, which was subsequently equipped with a stir bar, septum and reflux condenser connected to two gas washing flasks filled with sodium hydroxide (19.7 g, 0.49 mol) in water (250 mL). Freshly dried THF (300 mL) was added under nitrogen counter-flow suspending the sarcosine. After ensuring a gas-tight apparatus by checking nitrogen leaving through the gas washing bottles, the nitrogen stream was turned off. Diposgene (15.9 mL, 0.13 mol) was slowly added by syringe. The colourless suspension was heated to 70 °C under stirring, yielding a clear solution after 3 h. Then, the septum was exchanged with a quick-fit, fitted with a glass tube, through which a constant stream of nitrogen was bubbled through the solution for 3 hours, removing excess phosgene, hydrogen chloride and THF. The reaction mixture was stored at -80 °C overnight. Remaining THF was removed *in vacuo* until a brown solid was obtained. This solid was re-suspended in THF (60 mL) and precipitated to dry hexane (300 mL). The solution was cooled to -18 °C to complete precipitation and filtered under dry nitrogen atmosphere. The

precipitate was washed with hexane and dried in a constant stream of dry nitrogen. The next day, the product was dried in high vacuum in a sublimation apparatus for 2 h and subsequently sublimated at  $1 \times 10^{-3}$  bar at 80 °C. Colourless crystals were obtained in a yield of 60% (11.4 g, 99 mmol).

mp 103.3 °C (1 °C/min, starting at 95 °C)

$^1\text{H}$  NMR (400 MHz, DMSO- $d_6$ ):  $\delta$  [ppm] = 4.22 (2H, s,  $\text{CH}_2\text{-CO}$ ), 2.86 (3H, s, N- $\text{CH}_3$ ).

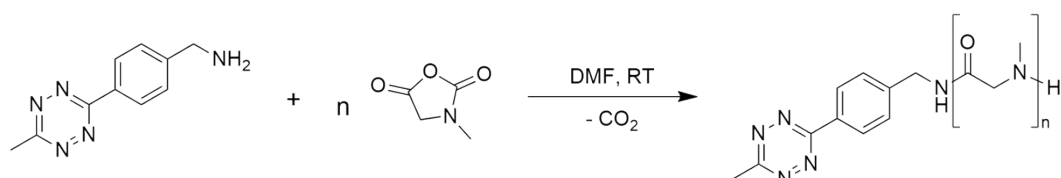
**$\gamma$ -Benzyl-L-glutamate N-carboxyanhydride.** The synthesis of  $\gamma$ -benzyl-L-glutamate (Glu(OBn)) NCA was carried out as previously reported.<sup>1</sup> H-Glu(OBn)-OH (10.1 g, 42.7 mmol) were thoroughly pestled and dried *in vacuo* in a flame-dried, 500 mL three-necked round bottom flask for 2 h. The flask was subsequently equipped with a stir bar, septum and reflux condenser connected to two gas washing flasks filled with sodium hydroxide (5.1 g, 0.13 mol) in water (250 mL). Freshly dried THF (200 mL) was added under nitrogen counter-flow suspending the amino acid. After ensuring a gas-tight apparatus by checking nitrogen leaving through the gas washing bottles, the nitrogen stream was stopped and diphosgene (4.1 mL, 34 mmol) was added slowly by syringe. The suspension was heated to 70 °C under stirring, yielding a clear and slightly yellow solution after 2 h. Then, the septum was exchanged with a quick-fit, fitted with a glass tube, through which a constant stream of nitrogen was bubbled through the solution for 3 h, removing excess phosgene, hydrogen chloride and THF. The reaction mixture was stored at -80 °C overnight. Remaining THF was removed *in vacuo* until a slightly yellow solid was obtained. The crude product was re-dissolved in 100 mL THF and recrystallised from THF/hexane (1:1) twice. Crystallisation was completed at -18 °C overnight and the product was filtered under dry nitrogen atmosphere,

washed with hexane and dried first under a stream of dry nitrogen and finally under high vacuum. Colourless crystals were obtained (8.6 g, 33 mmol, 76%).

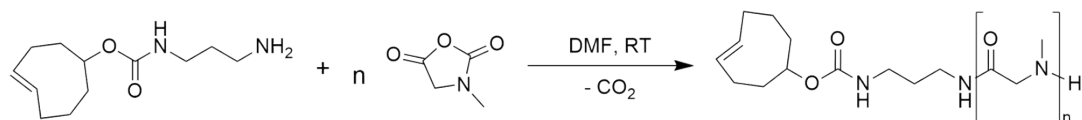
mp: 93.6 °C (1 °C/min, starting at 85 °C)

$^1\text{H}$  NMR (400 MHz,  $\text{DMSO}-d_6$ ):  $\delta$  [ppm] = 9.10 (s, 1H, CO-NH-CHR), 7.39-7.33 (m, 5H,  $\text{CH}_2\text{-C}_6\text{H}_5$ ), 5.10 (s, 2H,  $\text{CH}_2\text{-C}_6\text{H}_5$ ), 4.47 (ddd,  $J = 8.0$  Hz, 5.6 Hz, 1.2 Hz, 1H, NH-CH-CO), 2.52 (m, 2H,  $\text{CH}_2\text{-CH}_2\text{-CO}$ ), 2.10-1.88 (m, 2H,  $\text{CH}_2\text{-CH}_2\text{-CO}$ ).

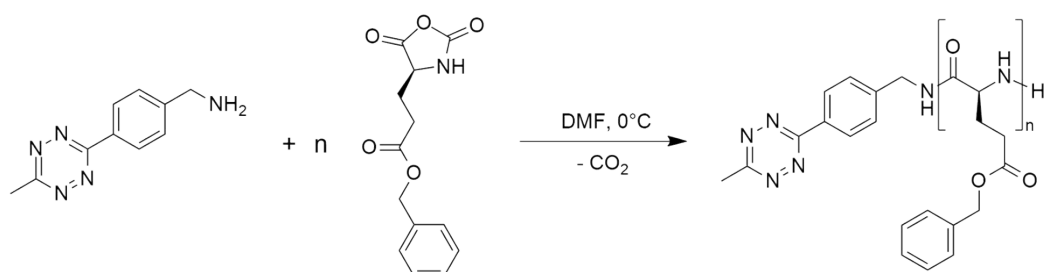
## 1.2. Polymer syntheses



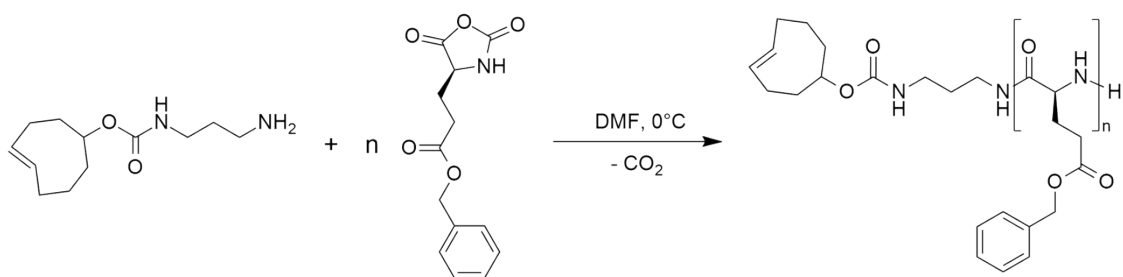
**Scheme S1.** Reaction scheme for the synthesis of mTz-pSar by ring-opening NCA polymerisation.



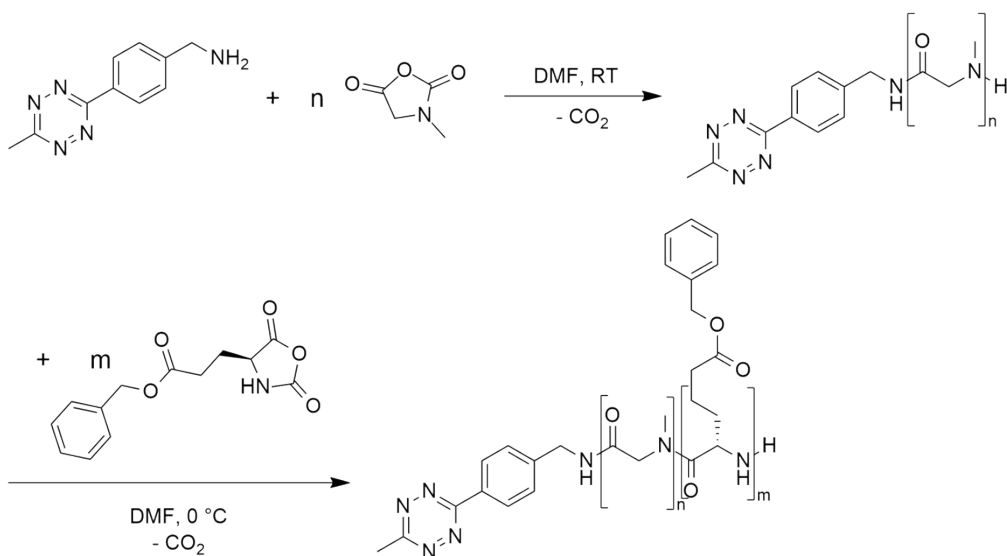
**Scheme S2.** Reaction scheme for the synthesis of TCO-pSar by ring-opening NCA polymerisation.



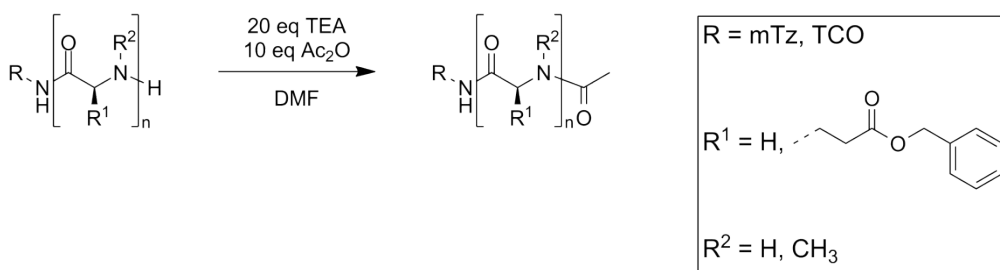
**Scheme S3.** Reaction scheme for the synthesis of mTz-pGlu(OBn) by ring-opening NCA polymerisation.



**Scheme S4.** Reaction scheme for the synthesis of TCO-pGlu(OBn) by ring-opening NCA polymerisation.

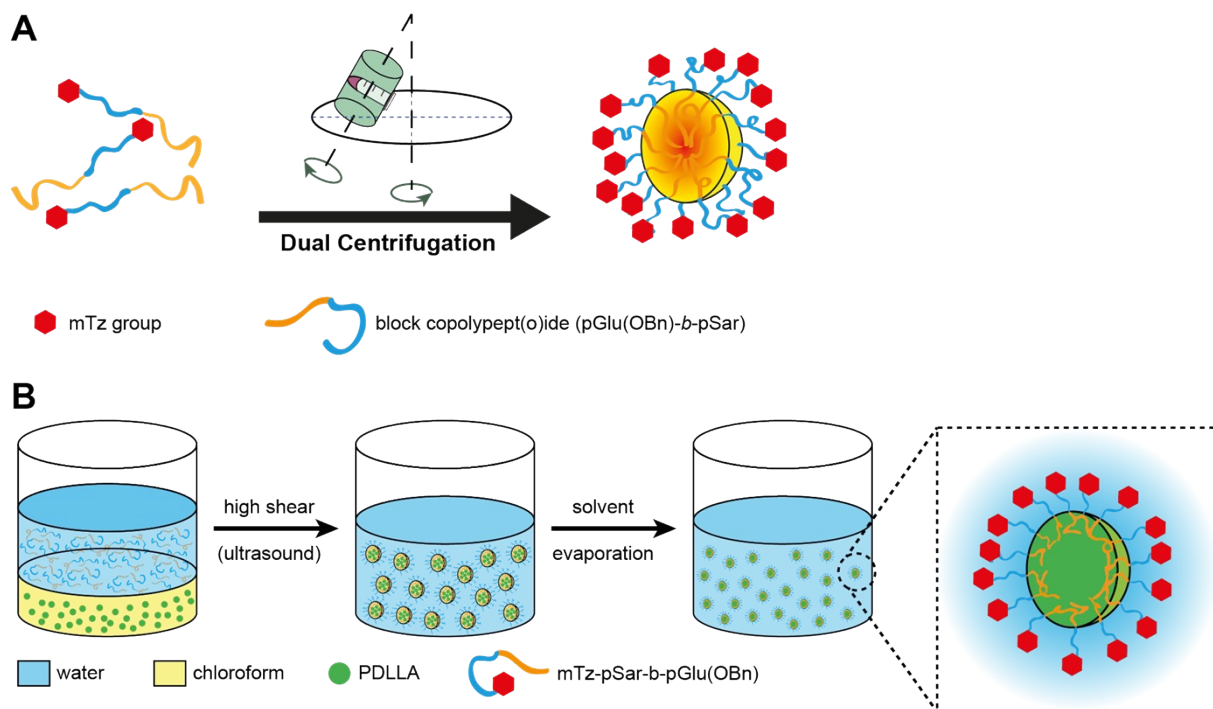


**Scheme S5.** Reaction scheme for the synthesis of mTz-pSar-*b*-pGlu(OBn) by sequential ring-opening NCA polymerisation.



**Scheme S6.** General reaction scheme for the acetylation of polymer end groups.

### 1.3. Nanoparticle preparation



**Scheme S7.** Schematic representations of nanoparticle preparations. A: Preparation of polymeric micelles by dual asymmetric centrifugation (DAC). B: Preparation of organic colloids by miniemulsion process in combination with solvent evaporation.

## 2. Supplementary analytical data

### 2.1. NMR data

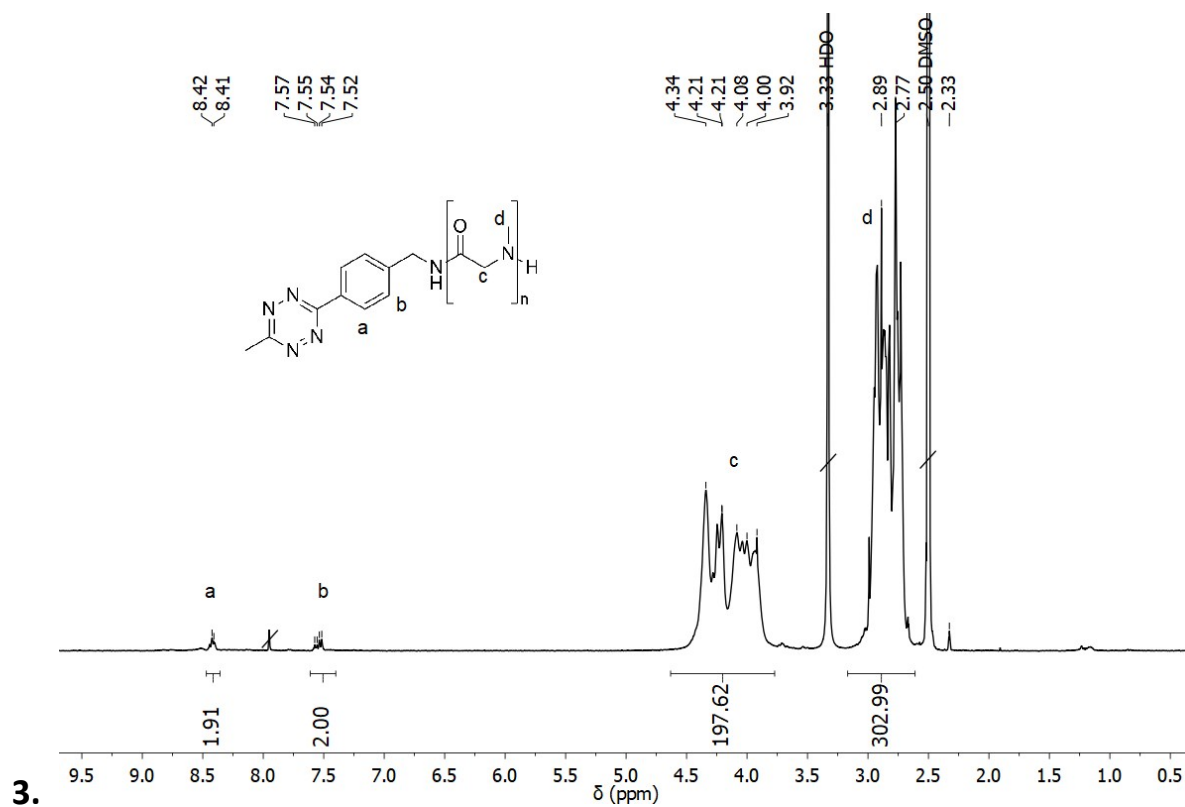


**Figure S1.** <sup>1</sup>H NMR spectrum of mTz-pSar<sub>99</sub> (**P3**) in DMSO-*d*<sub>6</sub> measured at 400 MHz.

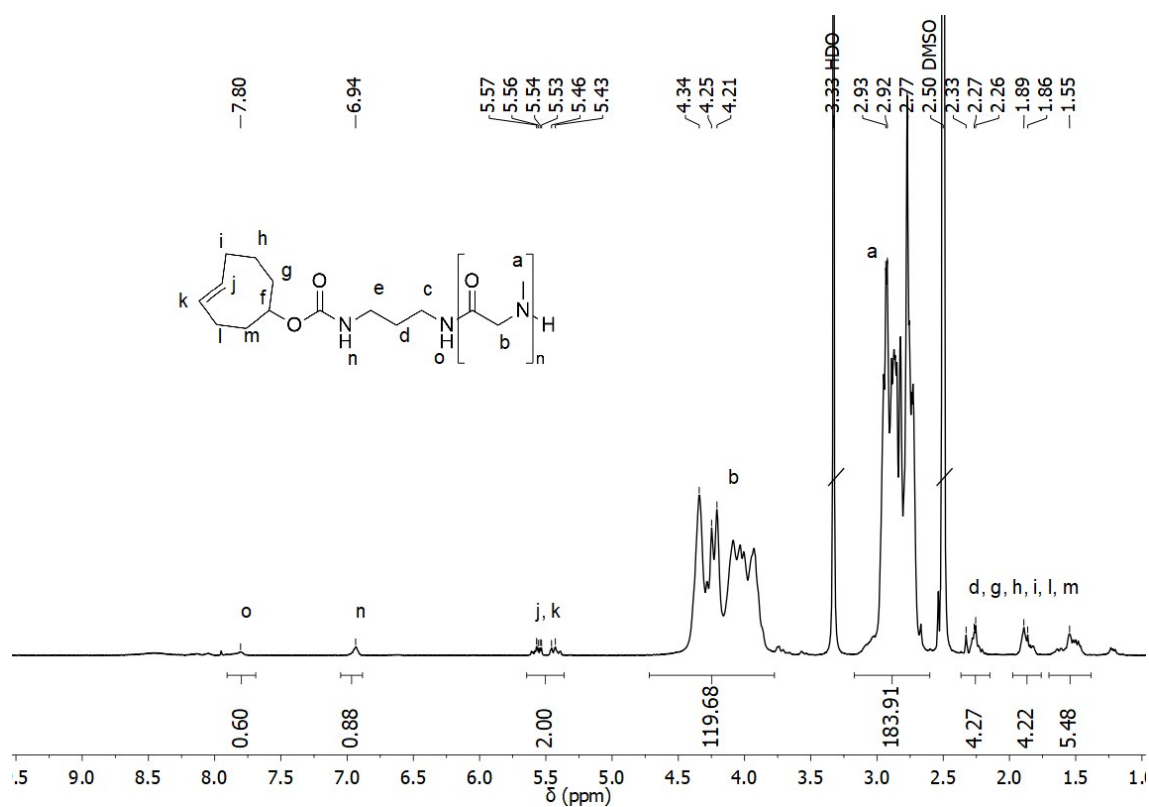


**Figure S2.** <sup>1</sup>H NMR spectrum of TCO-pSar<sub>66</sub> (**P5**) in DMSO-*d*<sub>6</sub> measured at 400 MHz.

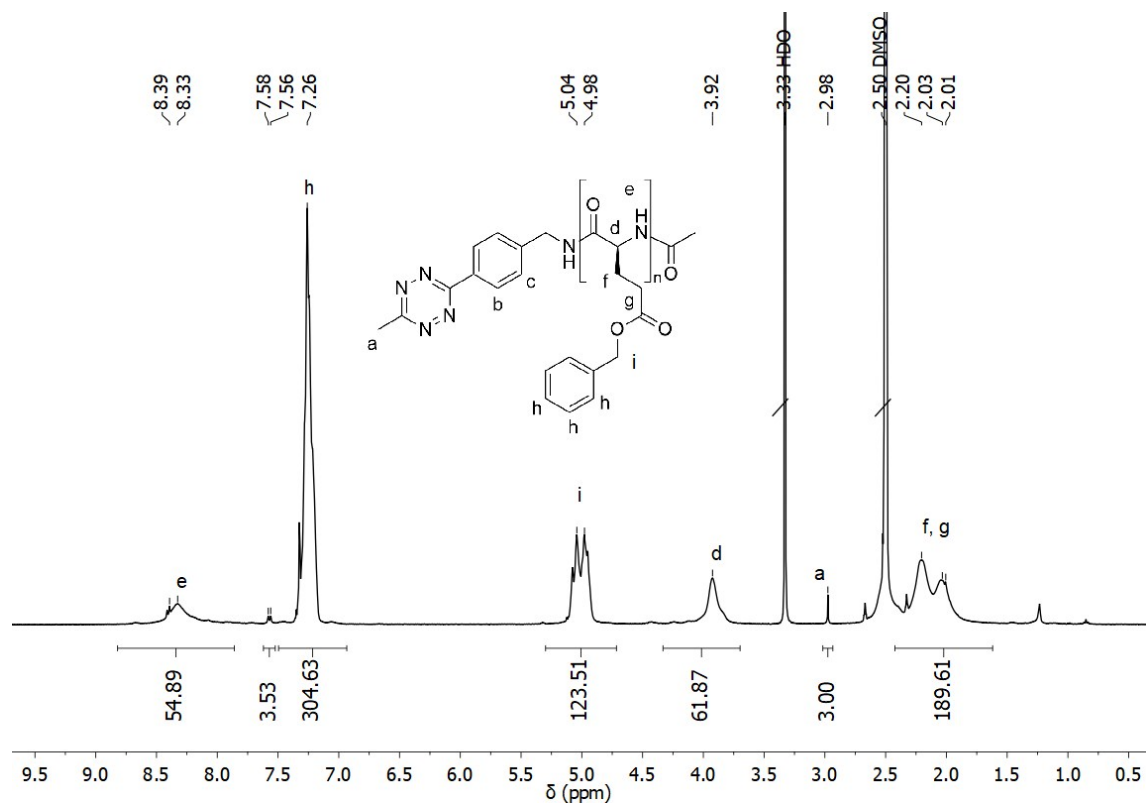


**Figure S3.** <sup>1</sup>H NMR spectrum of mTz-pGlu(OBn)<sub>62</sub> (**P9**) in DMSO-*d*<sub>6</sub> measured at 400 MHz.

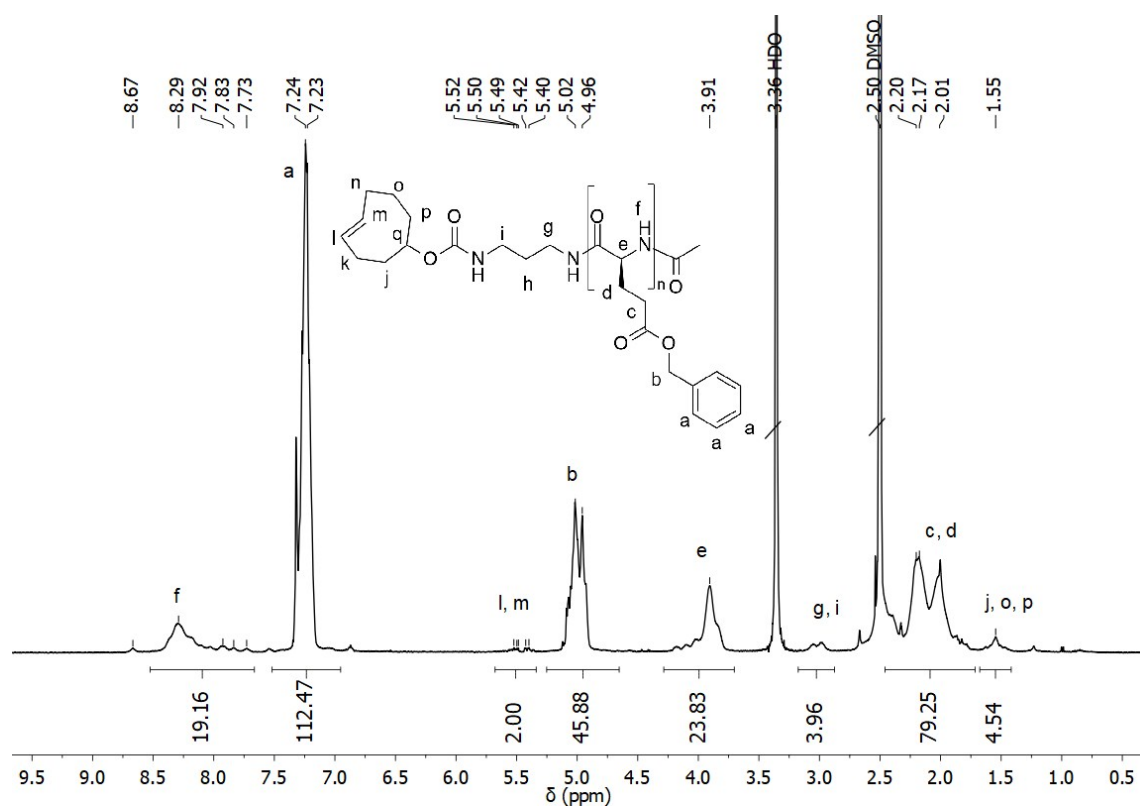


**Figure S4.**  $^1\text{H}$  NMR spectrum of TCO-pGlu(OBn) $_{23}$  (**P10**) in DMSO- $d_6$  measured at 400 MHz.

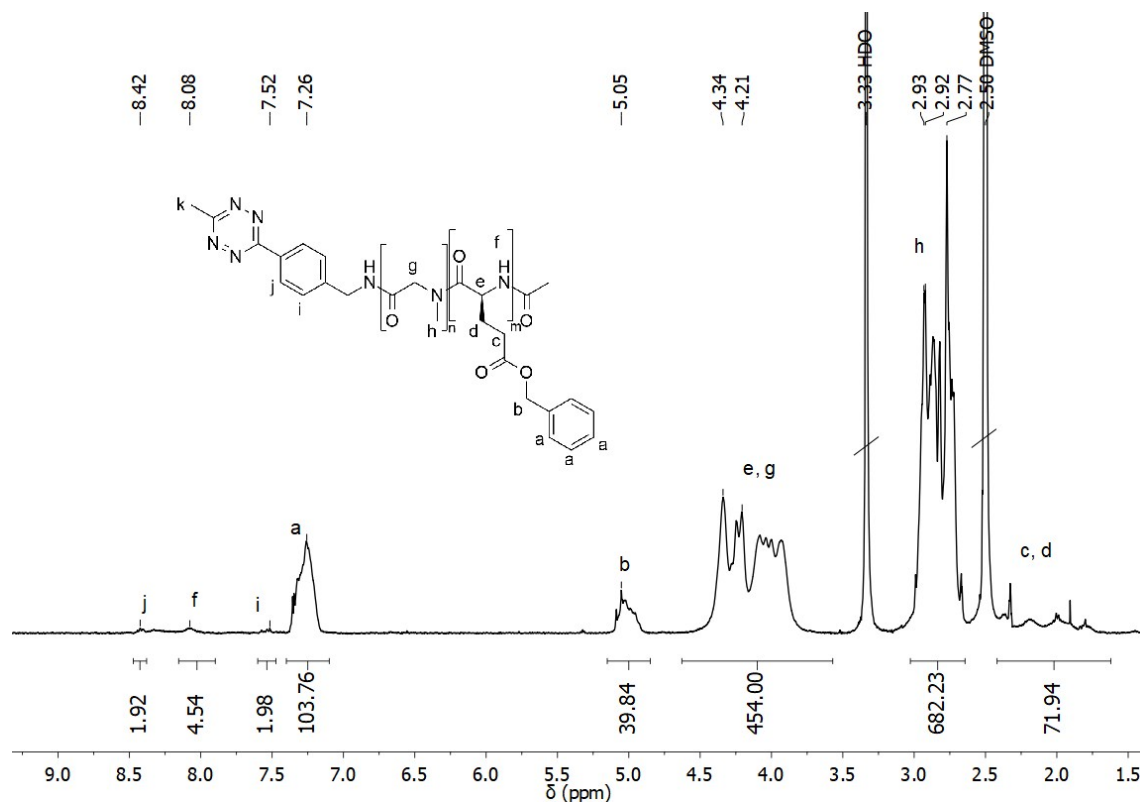


**Figure S5.**  $^1\text{H}$  NMR spectrum of mTz-pSar $_{217}$ -b-pGlu(OBn) $_{20}$  (**P12**) in DMSO- $d_6$  measured at 400 MHz.



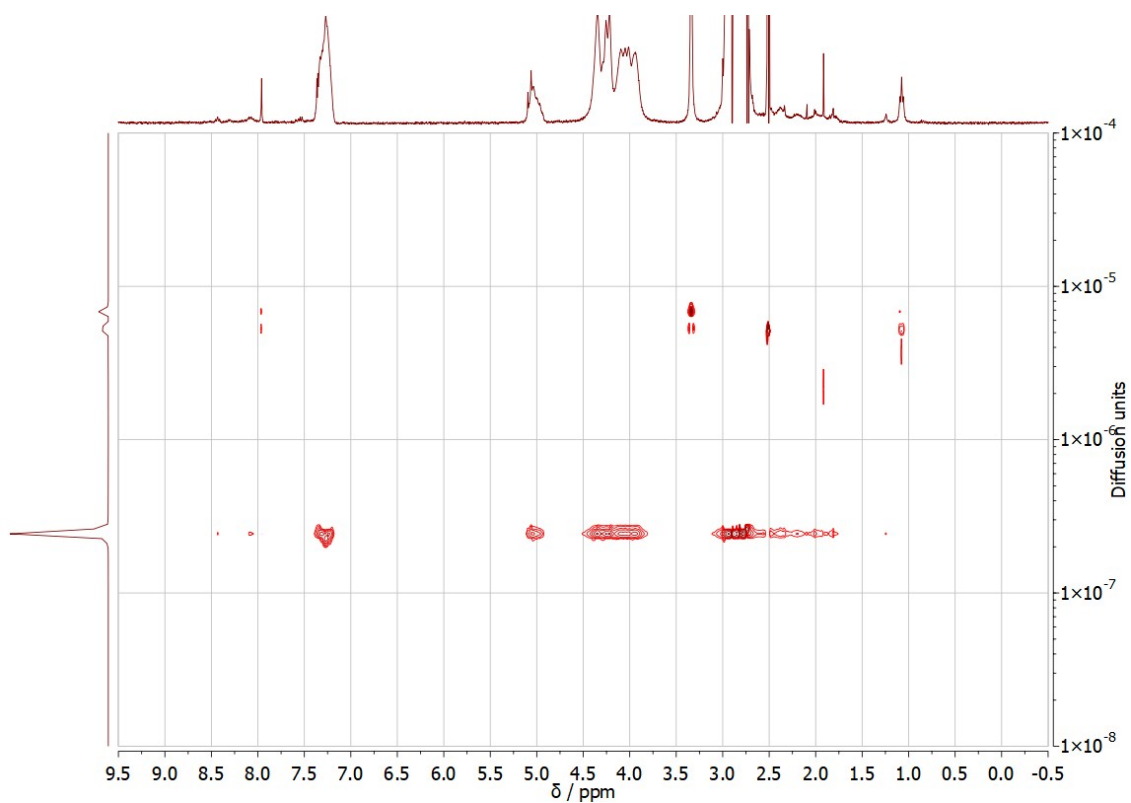


**Figure S6.** DOSY NMR spectrum of mTz-pSar<sub>217</sub>-*b*-pGlu(OBn)<sub>20</sub> (**P12**) in DMSO-*d*<sub>6</sub> measured at 400 MHz.

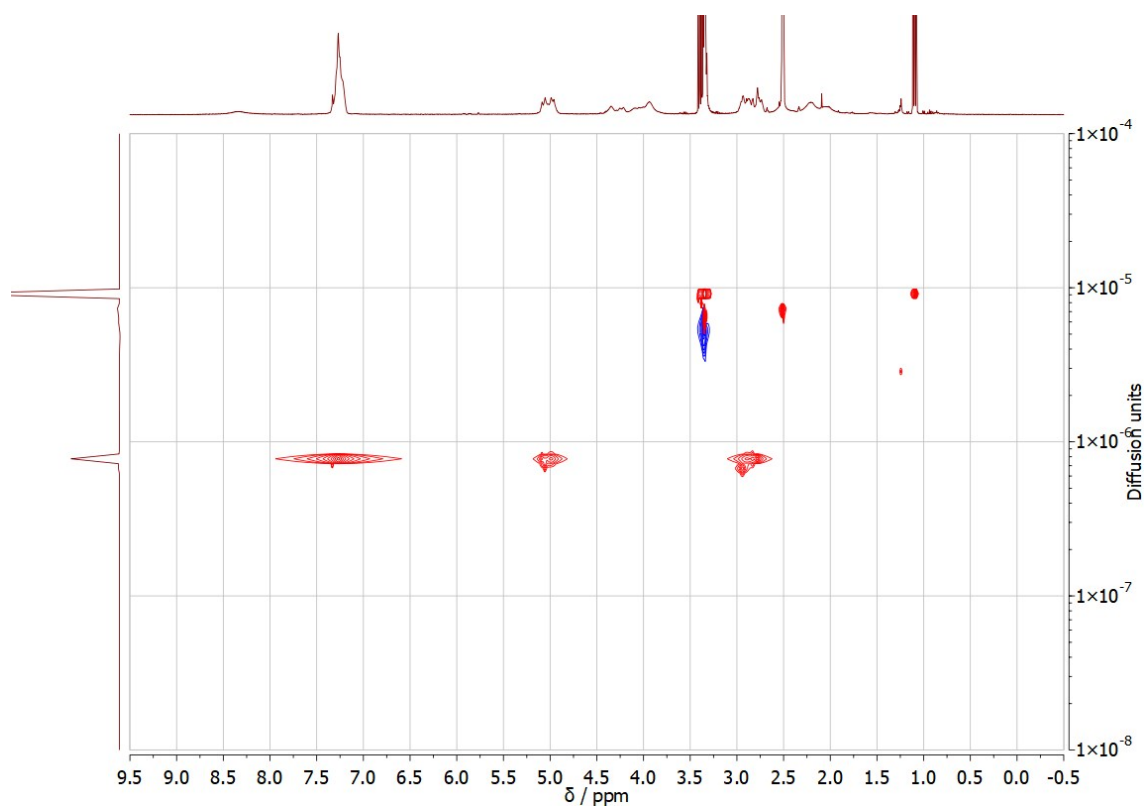


**Figure S7.** DOSY NMR spectrum of pSar<sub>99</sub>-*b*-pGlu(OBn)<sub>39</sub> obtained by reaction of **P3** with **P11** in DMSO-*d*<sub>6</sub> measured at 400 MHz.

### 3.1. GPC data

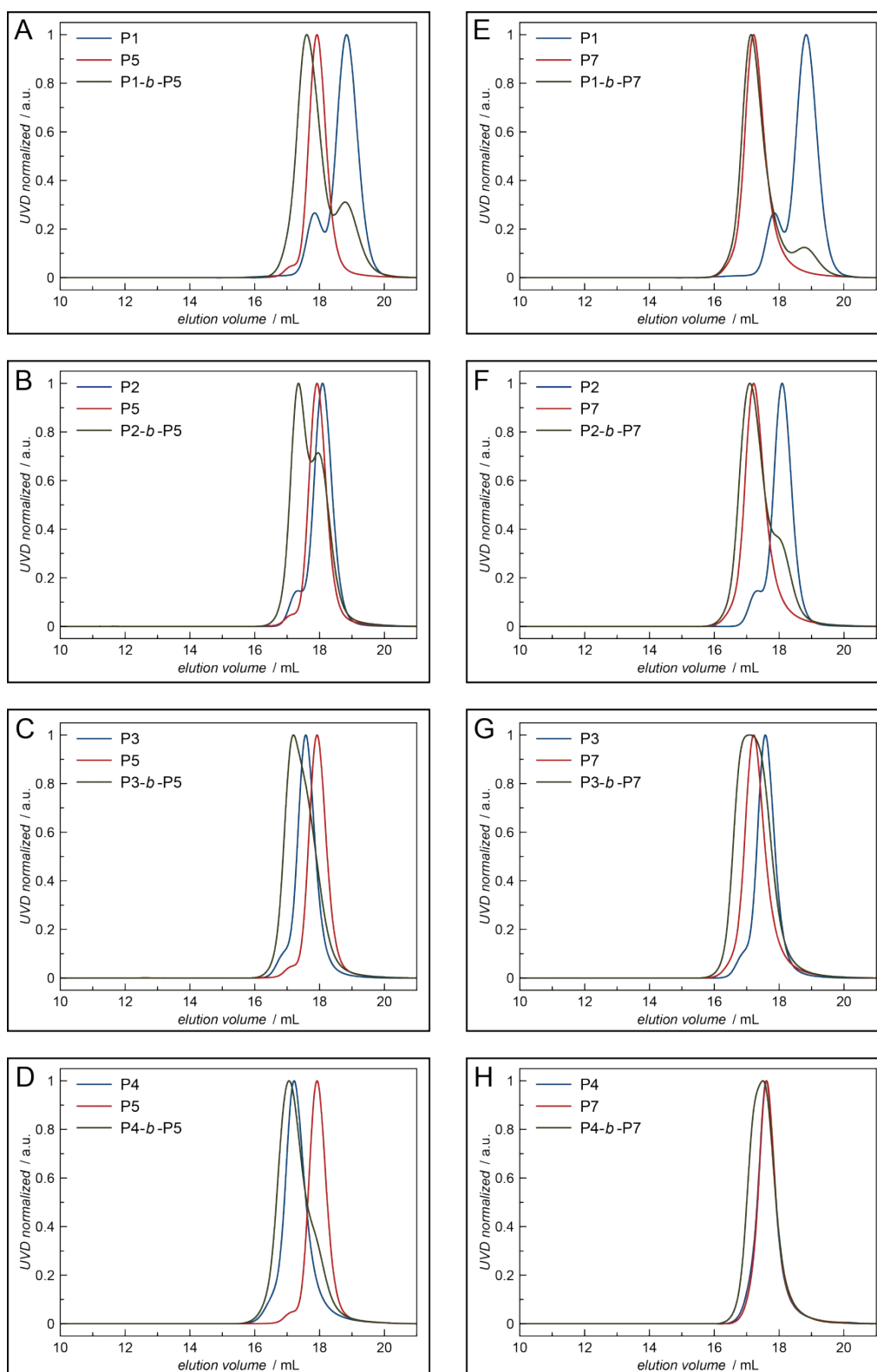


**Figure S8.** HFIP GPC elugrams (vs. PMMA standards) of the tetrazine ligation products of mTz-pSar polymers **P1-P4** with TCO-pSar polymers **P5** and **P7** and of the corresponding homopolymers.

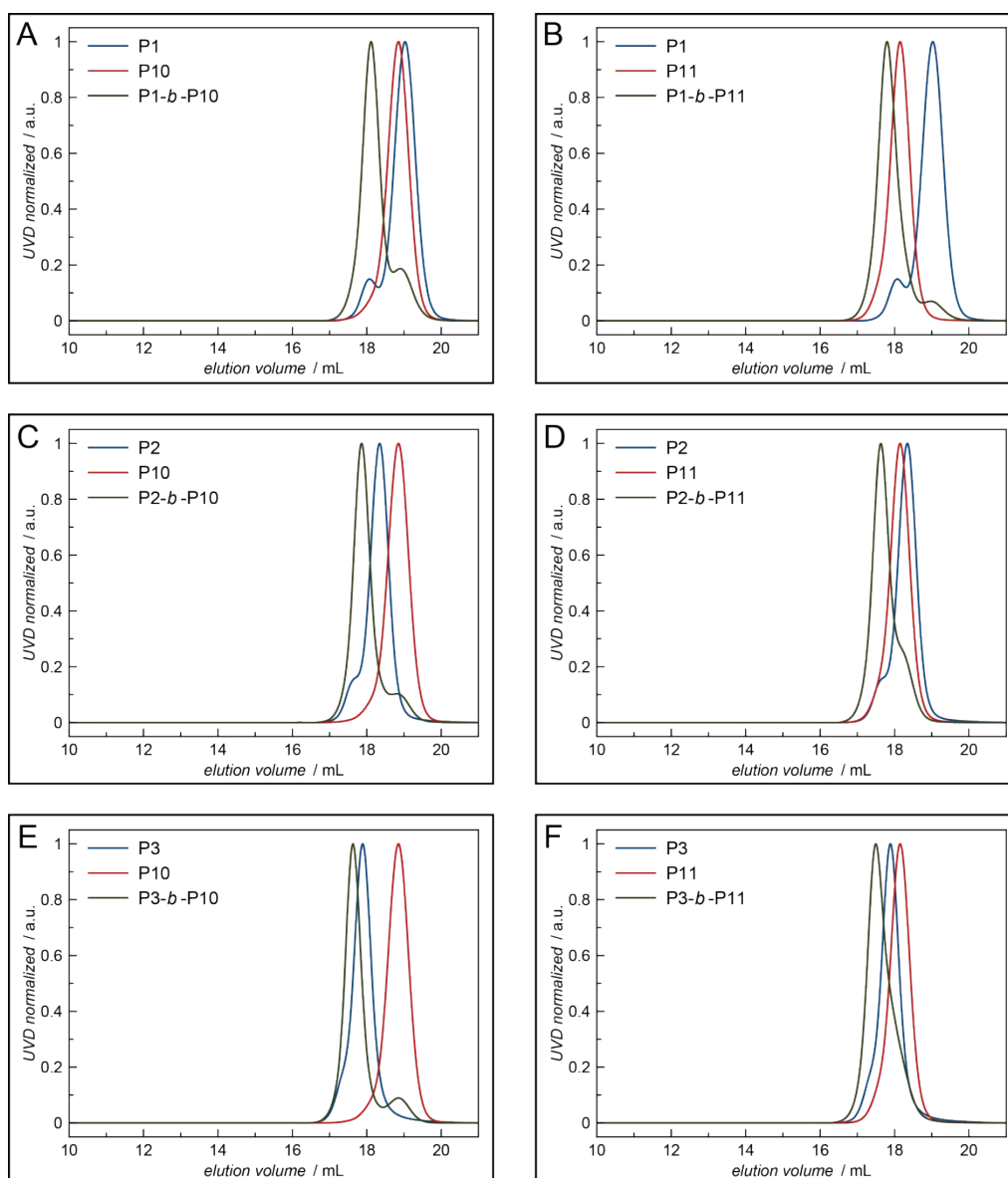


**Figure S9.** HFIP GPC elugrams (vs. PMMA standards) of tetrazine ligation products of mTz-pSar polymers **P1-P3** with TCO-pGlu(OBn) polymers **P10** and **P11** and of the corresponding homopolymers.

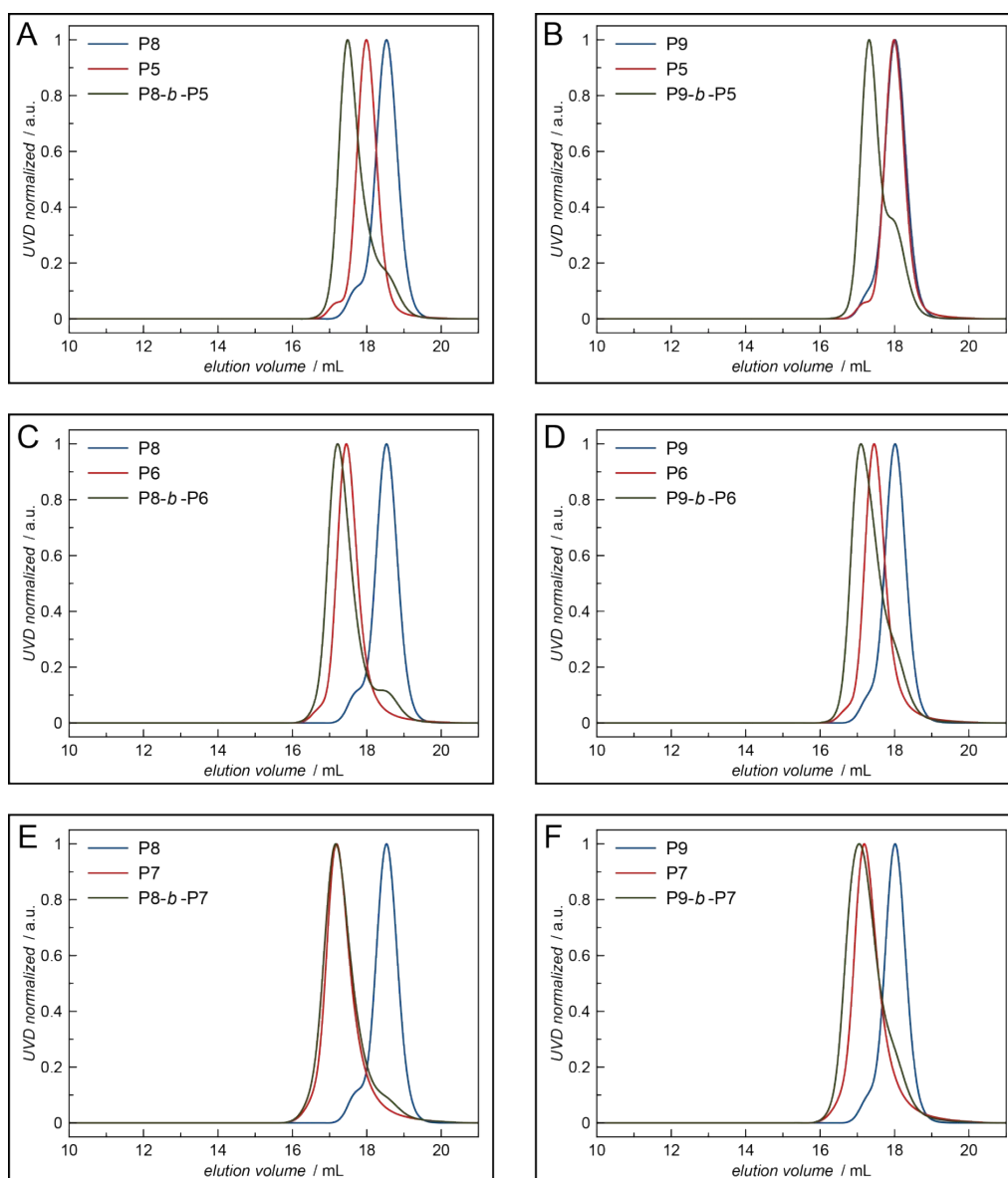


**Figure S10.** HFIP GPC elugrams (vs. PMMA standards) of the tetrazine ligation products of TCO-pSar polymers **P5-P7** with mTz-pGlu(OBn) polymers **P8** and **P9** and of the corresponding homopolymers.

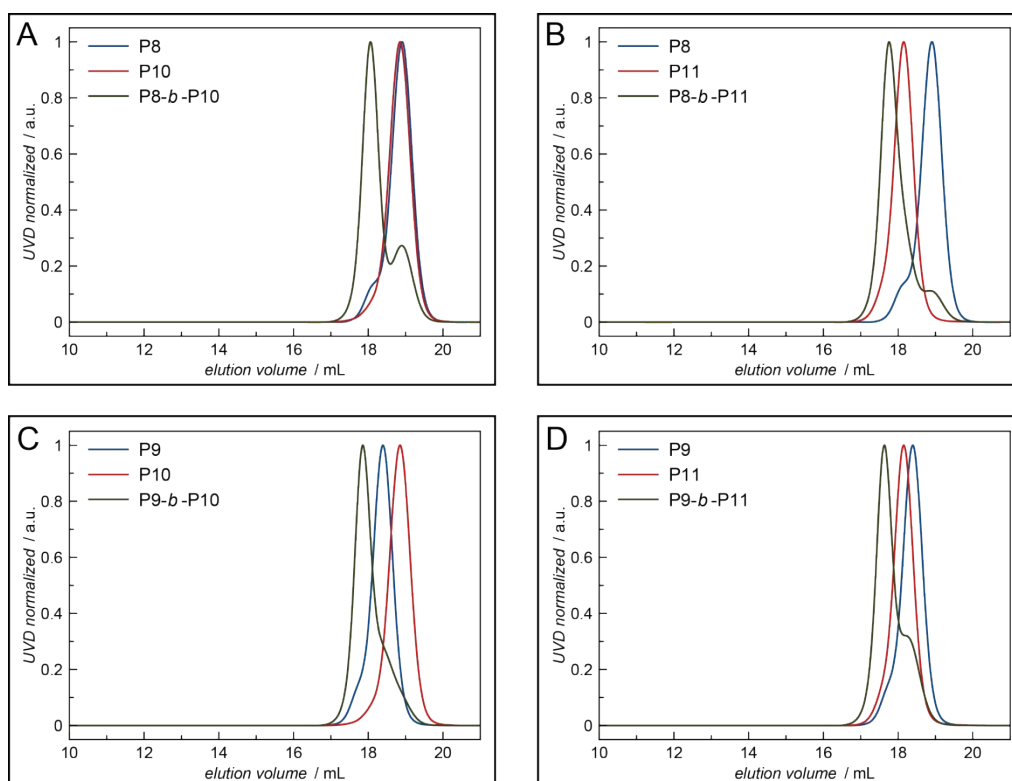


**Figure S11.** HFIP GPC elugrams (vs. PMMA standards) of tetrazine ligation products of mTz-pGlu(OBn) polymers **P8-P9** with TCO-pGlu(OBn) polymers **P10-P11** and of the corresponding homopolymers.

### 3.2. MALDI-TOF data

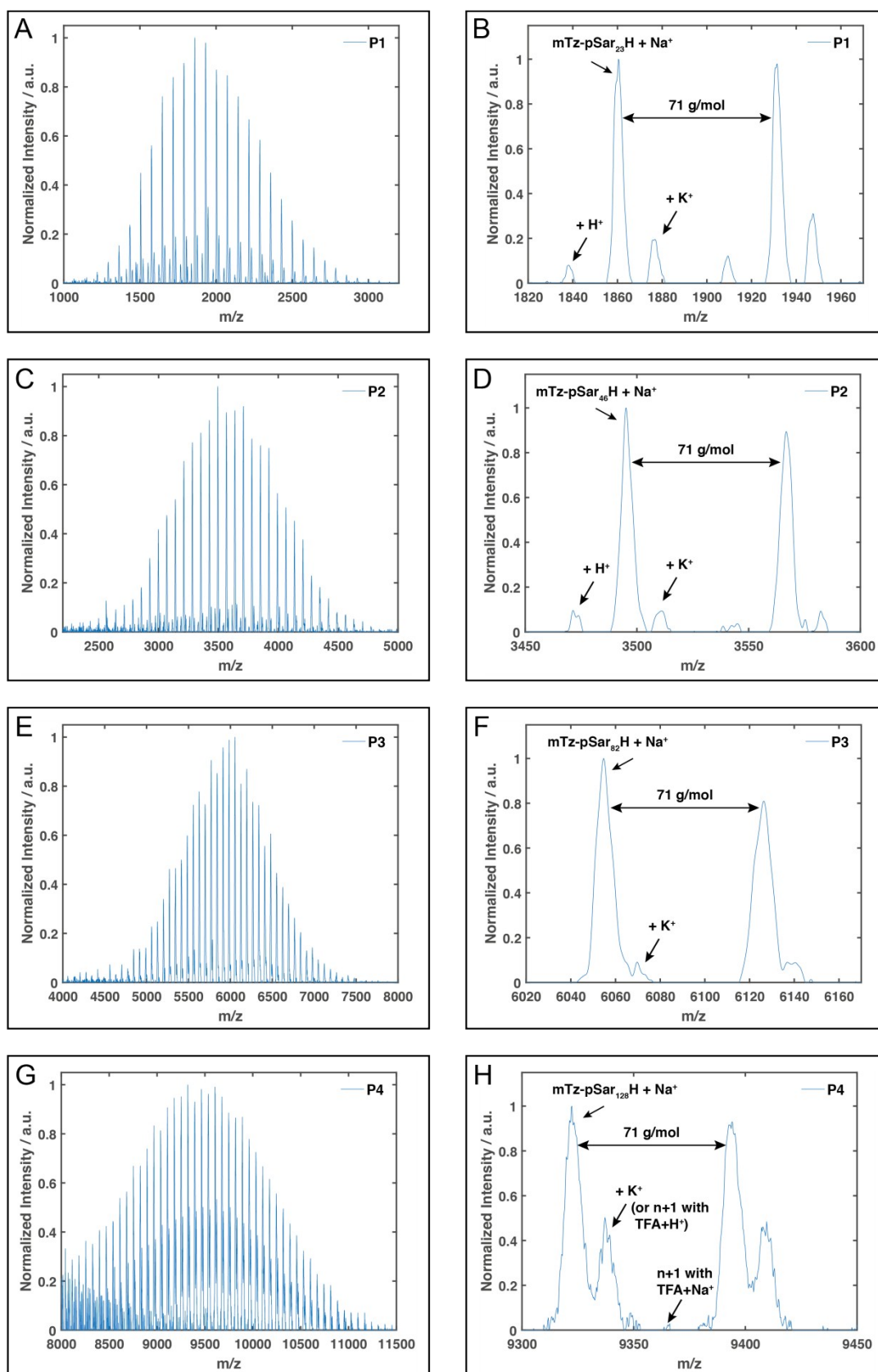


**Figure S12.** MALDI-TOF spectra of mTz-pSar polymers **P1** (A and B (Zoom)), **P2** (C and D (Zoom)), **P3** (E and F (Zoom)) and **P4** (G and H (Zoom)).

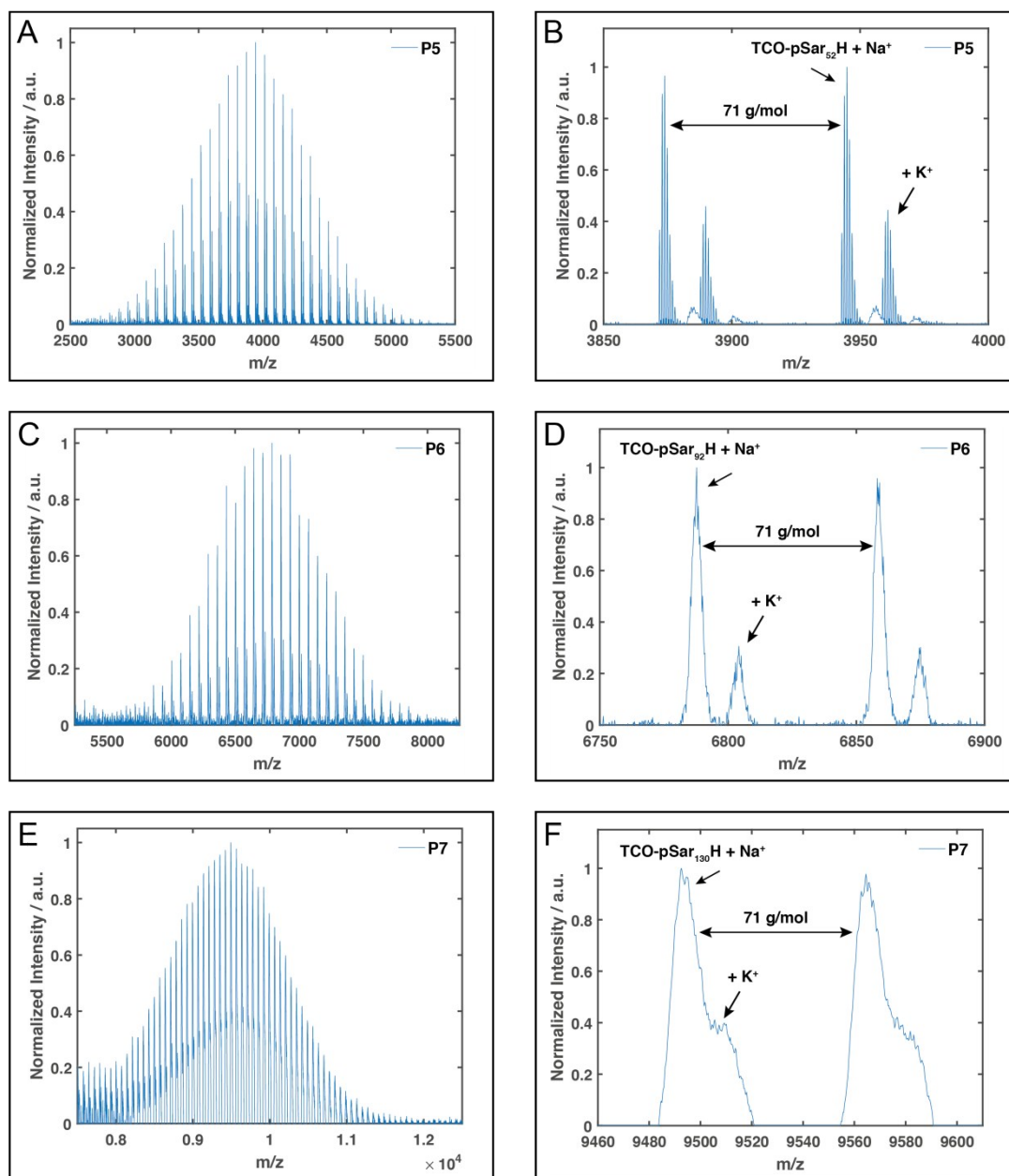


**Figure S13.** MALDI-TOF spectra of TCO-pSar polymers **P5** (A and B (Zoom)), **P6** (C and D (Zoom)) and **P7** (E and F (Zoom)).

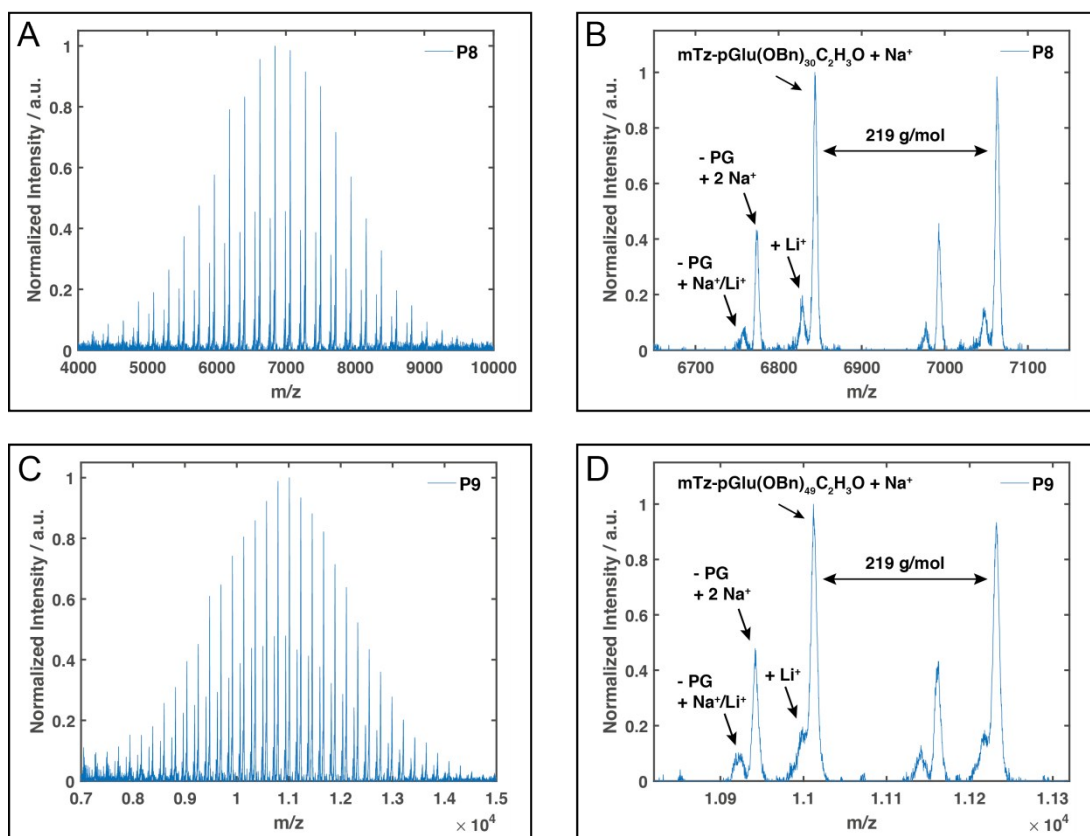


**Figure S14.** MALDI-TOF spectra of mTz-pGlu(OBn) polymers **P8** (A and B (Zoom)) and **P9** (C and D (Zoom)).

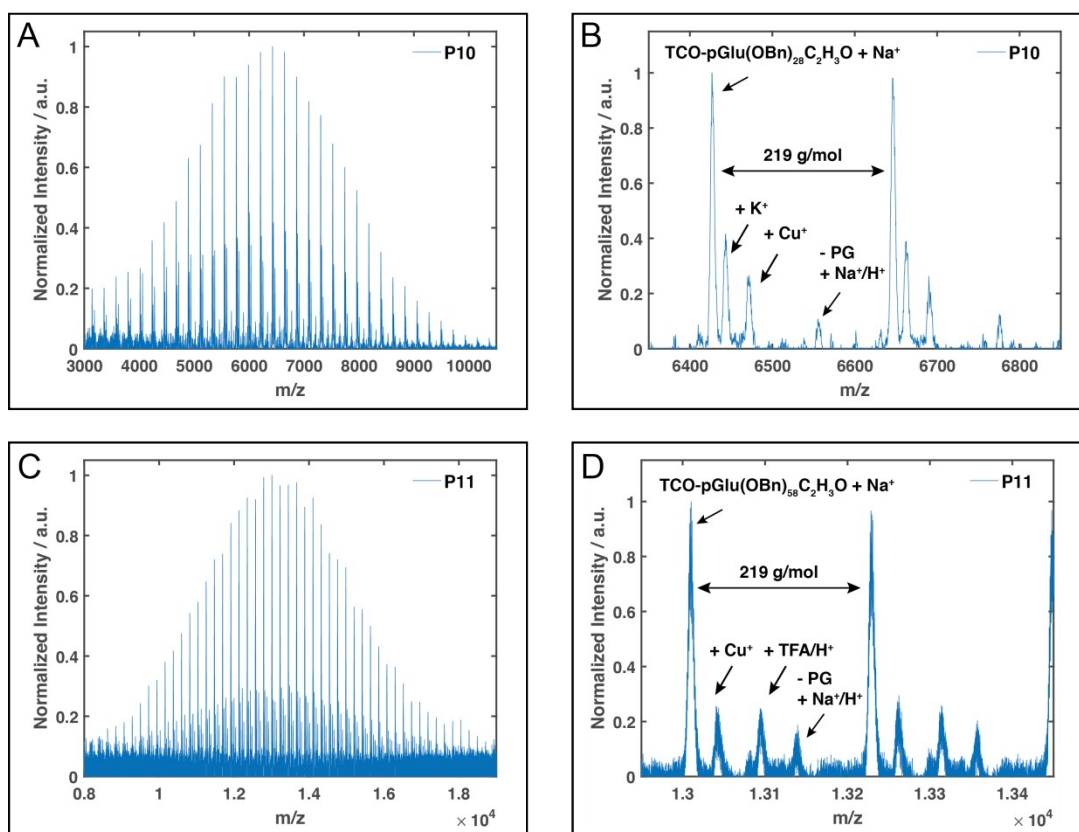


**Figure S15.** MALDI-TOF spectra of TCO-pGlu(OBn) polymers **P10** (A and B (Zoom)) and **P11** (C and D (Zoom)).



**Table S1.** Overview of MALDI-TOF data of the synthesised mTz- and TCO-functionalised polymers.

	Polymer	Initiator	$X_n(\text{target})$	$X_n(\text{MALDI})^*$	$\bar{D}_{(\text{MALDI})}^{**}$
P1	pSar	mTz-NH <sub>2</sub>	25	23	1.03
P2	pSar	mTz-NH <sub>2</sub>	50	46	1.01
P3	pSar	mTz-NH <sub>2</sub>	100	82	1.01
P4	pSar	mTz-NH <sub>2</sub>	200	128	1.00
P5	pSar	TCO-NH <sub>2</sub>	50	52	1.01
P6	pSar	TCO-NH <sub>2</sub>	100	92	1.01
P7	pSar	TCO-NH <sub>2</sub>	200	130	1.01
P8	pGlu(OBn)	mTz-NH <sub>2</sub>	30	30	1.02
P9	pGlu(OBn)	mTz-NH <sub>2</sub>	60	49	1.02
P10	pGlu(OBn)	TCO-NH <sub>2</sub>	25	28	1.05
P11	pGlu(OBn)	TCO-NH <sub>2</sub>	50	58	1.02

\* $X_n(\text{MALDI})$  indicates the highest peak observed in the MALDI spectrum. \*\* Calculated from the observed peaks using MATLAB.

### 3.3. Tetrazine ligation kinetics

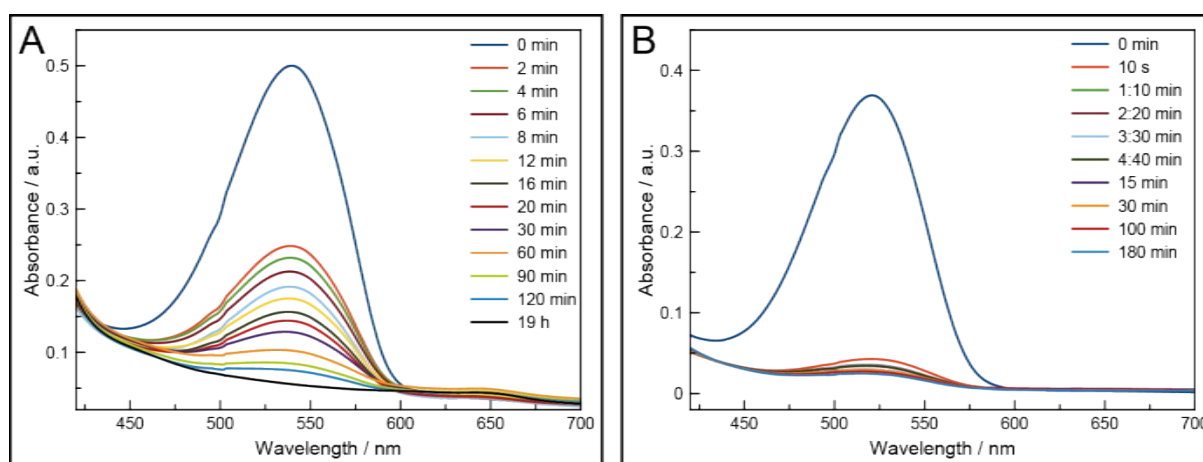


**Figure S16.** Measurements of the tetrazine ligation reaction kinetics between **P4** and **P7** by UV-Vis spectroscopy in DMF (A) and water (B).

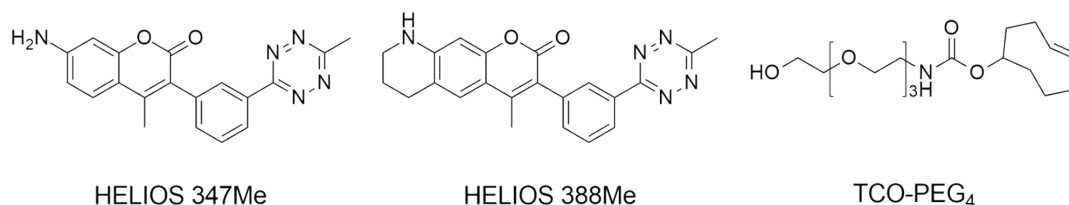


**Figure S17.** Chemical structures of the fluorogenic “turn-on” Tz derivatives HELIOS 347Me and HELIOS 388Me<sup>2</sup> and TCO-PEG<sub>4</sub> used for kinetic measurements.

## References

- 1 A. Birke, D. Huesmann, A. Kelsch, M. Weilbacher, J. Xie, M. Bros, T. Bopp, C. Becker, K. Landfester and M. Barz, *Biomacromolecules*, 2014, **15**, 548–557.
- 2 L. G. Meimetis, J. C. T. Carlson, R. J. Giedt, R. H. Kohler and R. Weissleder, *Angewandte Chemie (International ed. in English)*, 2014, **53**, 7531–7534.